Check for updates

Hindawi
Adsorption Science & Technology
Volume 2022, Article ID 7384924, 13 pages
https://doi.org/10.1155/2022/7384924

Research Article

Thermodynamics and Mechanism of the Adsorption of Heavy Metal Ions on Keratin Biomasses for Wastewater Detoxification

Salaudeen Abdulwasiu Olawale,[1] Adrián Bonilla-Petriciolet,[2] Didilia Ileana Mendoza-Castillo,[2,3] Chibueze Charles Okafor,[4] Lotfi Sellaoui,[5] and Michael Badawi[6]

[1]*Chemistry Unit of Applied Mathematics Programme, National Mathematical Centre Abuja, Nigeria*
[2]*Chemical Engineering Department, Instituto Tecnológico de Aguascalientes, Aguascalientes 20256, Mexico*
[3]*CONACYT, Cátedras Jóvenes Investigadores, 03940, Mexico*
[4]*Chemistry Department, University of Abuja, Nigeria*
[5]*Laboratory of Quantum and Statistical Physics, LR18ES18, Monastir University, Faculty of Sciences of Monastir, Tunisia*
[6]*Laboratoire de Physique et Chimie Théoriques, UMR 7019–CNRS, Université de Lorraine, Nancy F-54000, France*

Correspondence should be addressed to Adrián Bonilla-Petriciolet; petriociolet@hotmail.com and Michael Badawi; michael.badawi@univ-lorraine.fr

Received 28 September 2021; Revised 7 February 2022; Accepted 22 February 2022; Published 19 March 2022

Academic Editor: Silvano Mignardi

Copyright © 2022 Salaudeen Abdulwasiu Olawale et al. This is an open access article distributed under the Creative Commons Attribution License, which permits unrestricted use, distribution, and reproduction in any medium, provided the original work is properly cited.

The analysis of thermodynamics and mechanism of the adsorption of cadmium, chromium, copper, and lead ions from aqueous solution with two keratin-based biomaterials, namely, human hair and sheep fur, is reported in this paper. The effect of initial ion concentration, temperature, pH, contact time, and biomaterial amount on the removal of these heavy metal ions using these keratinous adsorbents was studied. The adsorption of heavy metal ions was highly dependent on the operating parameters where pH and temperature showed the highest impact. Maximum adsorption capacities of these biomaterials were up to 1.33 and 1.40 mmol/g for chromium ions using human hair and sheep fur, respectively. Adsorption kinetic rates of tested heavy metal ions were calculated via a pseudo-second-order model, and they ranged from 0.054 to 0.261 g/mmol·min. A detailed thermodynamic analysis of lead ion adsorption was performed showing an endothermic removal of this adsorbate with both human hair and sheep fur with adsorption enthalpies of 84.5 and 97.1 kJ/mol, respectively. Statistical physics calculations demonstrated that this heavy metal ion was adsorbed via a multi-interaction mechanism especially for human hair. These keratinous biomaterials showed competitive adsorption capacities especially for chromium ion removal and can outperform commercial activated carbons and other adsorbents reported in literature.

1. Introduction

The earth is made up of about 70% water with only about 3% being freshwater mostly found as polar ice and underground aquifers. The surface freshwater in rivers, lakes, and other reservoirs is estimated less than 0.25% of the total available amount worldwide [1]. In the last decades, the rapid industrialization in metallurgy, power plants, oil processing, mining, paints, and other important industrial sectors has generated an increment of the discharges of harmful heavy metals into the water bodies [2]. Natural sources (e.g., weathering of rocks and minerals, volcanic activities, and soil erosion) also contribute to the heavy metal pollution. Several studies have confirmed that heavy metals are toxic to different life forms (e.g., plants, aquatic organisms, and humans) and can generate a significant environmental impact. Mercury, copper, arsenic, chromium, cadmium, and lead are examples of toxic heavy metals in the context of environmental protection [3]. These metals are nonbiodegradable and toxic if a chronic

exposure occurs even at low concentrations and can persist in nature thus causing their bioaccumulation via food and/or drinking water [4–6]. For instance, copper and zinc are required by humans at low dose, but they are toxic at concentrations higher than 1 mg/L, as stated by the World Health Organization [7–10].

The detoxification of wastewaters polluted by heavy metals is fundamental to protect the environment and public health [11], and consequently, it is a current research topic [12]. Different treatment technologies have been applied to face the pollution caused by heavy metals such as coagulation and flocculation [13, 14], ion exchange [15, 16], advanced oxidation [17–19], membrane filtration [20–23], electrochemical degradation [24–26], and biodegradation. These techniques could imply economical and/or technical disadvantages including low removal effectiveness at high metal concentrations, colateral generation of toxic residues, high sensitivity to operating conditions, long processing time, application of expensive chemicals and supplies, high energy consumption, and capital investment [27]. Different studies have been performed to overcome these deficiencies and to achieve an effective reduction of the concentration of these pollutants in treated effluents.

Adsorption is a cost-effective method to detoxify fluids polluted by heavy metals [28, 29]. This separation process implies the transfer of adsorbate (i.e., pollutant) from the fluid (i.e., water or industrial effluent) to the surface of a solid matrix (i.e., adsorbent) that should have a tailored surface chemistry and porosity to reach an effective separation. It also offers the possibility to recover the adsorbate(s) loaded on the adsorbent surface via desorption thus facilitating the adsorbent recycling [30]. The effectiveness of adsorption of heavy metal ions is affected by several operating variables like contact time, adsorbent amount, temperature, initial metal concentration, and pH [31]. Also, textural parameters and surface functionalities of the material used as an adsorbent are paramount to achieve a successful removal of these pollutants. Therefore, it is important to characterize, assess, and model the performance of low-cost materials as adsorbents for the removal of heavy metal ions at different operating conditions with the aim of identifying the best alternatives for real-life and industrial applications.

In particular, a large number of low-cost adsorbents have been studied and, in less extent, some of them have been commercialized for removing heavy metal ions from water [32]. These adsorbents can be obtained from mineral, organic, or biological sources [33]. Keratinous materials from biological origin like human hair (HH), sheep fur (SF), and chicken feathers can be employed as alternative adsorbents of these pollutants in their native forms or after an activation procedure that implies their surface functionalization. These biomaterials can be effective in the removal of heavy metal ions due to their high stability, water insolubility, intricate networks, and surface rich in functional groups like hydroxyl, carboxyl, amino, and sulphur [34]. Therefore, the utilization and valorization of biomaterials are an alternative to reduce the operational costs of wastewater treatment and to develop effective and sustainable adsorption processes.

In this manuscript, the study of mechanism and thermodynamics of the adsorption of copper (Cu^{2+}), chromium (Cr^{6+}), cadmium (Cd^{2+}), and lead (Pb^{2+}) ions on HH and SF is reported. These biomaterials have been studied in their native form to analyze and characterize the adsorption properties of these ions and to calculate kinetic and thermodynamic parameters that allowed the interpretation and understanding of the corresponding adsorption mechanisms. These findings are the main contribution and novelty of this paper. As stated, these biomaterials are low-cost and renewable and offer the possibility to be used as raw adsorbents and feedstock to prepare composites and new materials for the removal of water pollutants. Finally, statistical physics calculations were also performed to interpret and explain the adsorption mechanism of these heavy metal ions using these keratin-based biomaterials where Pb^{2+} ion was utilized as a representative adsorbate of this type of relevant inorganic pollutants.

2. Methodology

2.1. Description of Keratin-Based Biomaterials and Their Characterization. HH and SF were the keratin-containing biomaterials utilized as adsorbents. The HH sample was washed with deionized water and detergent and dried at 298 K. The experimental tests of adsorption of heavy metal ions were done with a HH sample length < 2 mm. SF was collected from a Fulani settlement in Kwali Area Council of the Federal Capital Territory Abuja FCT, and these samples were handled in the same way as the case of HH.

Specific moisture content, ignition mass loss, pH, and bulk density were quantified for these biomaterials using standard procedures [4]. Functional groups of the surfaces of both HH and SF were analyzed via FTIR at room temperature, and results were used to identify their role for the removal of heavy metal ions. Absorption spectra were recorded at 4000–400 cm^{-1} wavenumber with 4 cm^{-1} resolution and 45 scans using a Shimadzu FTIR-8400S equipment. SEM micrographs of both HH and SF were recorded before and after the adsorption at different magnifications to analyze their surface morphology with a JEOL JSM 6100 equipment.

2.2. Adsorption Experiments. The adsorption of heavy metal ions on HH and SF was assessed at different conditions of pH (1–5), adsorbent dosage W/V (0.2-4 g/L), initial metal ion concentration C_i (mmol/L), and contact time t (10–360 min) at 298 K. Equilibrium studies were also performed at 293–323 K and pH 4 to analyze the adsorption thermodynamics. All removal tests were done with batch adsorbers properly stirred at 270 rpm. Double-distilled water and analytical grade reagents were utilized to prepare all the required solutions, while pH adjustment was done with HNO_3 (0.1 M) and NaOH (0.1 M). The concentrations of Cu^{2+}, Cr^{6+}, Cd^{2+}, and Pb^{2+} ions were quantified with atomic absorption spectroscopy, and the biomaterial performance was analyzed considering the adsorption capacity (q, mmol/g)

$$q = \frac{(C_i - C_f) \times V}{W}, \quad (1)$$

where C_f is the residual concentration (mmol/L) quantified for the heavy metal ion in the aqueous solution after adsorption at given operating conditions. Adsorption capacities of both kinetic and equilibrium studies for all heavy metal ions and two biomaterials were calculated with equation (1).

2.3. Adsorption Modeling and Statistical Physics Calculations. The rates of adsorption of these heavy metal ions on SF and HH were calculated with the pseudo-second- and pseudo-first-order models [35]. The pseudo-first-order model is described with the following expression:

$$q_t = q_e \left(1 - e^{-k_1 t}\right), \quad (2)$$

where q_e and q_t (mmol/g) are the adsorption capacities at equilibrium and at time t (min), respectively, and k_1 is the adsorption rate constant (min^{-1}). The pseudo-second-order equation is given by the following expression:

$$q_t = \frac{q_e^2 k_2 t}{1 + q_e k_2 t}, \quad (3)$$

where k_2 is the corresponding adsorption rate constant (g/mmol·min). Interested readers can found the explanation and fundaments of these kinetic models in the review [35]. A nonlinear regression was performed, and a comparison of the performance of these models was also done.

Thermodynamic parameters for the adsorption of Pb^{2+} ions with both keratin-based biomaterials were calculated using the van't Hoff equation [36]. In particular, the changes of entropy (ΔS^0), enthalpy (ΔH^0), and free energy (ΔG^0) of the adsorption of Pb^{2+} ion on HH and SF were calculated using the next equations [36–39]:

$$\begin{aligned} \Delta G^0 &= \Delta H^0 - T\Delta S^0, \\ \Delta G^0 &= -RT \ln K_d, \\ \ln K_d &= \frac{\Delta S^o}{R} - \frac{\Delta H^o}{RT}, \end{aligned} \quad (4)$$

where T is the adsorption temperature (K), R is the universal gas constant (8.314 J/mol K), and K_d is the adsorption equilibrium constant calculated from the experimental Pb^{2+} ion adsorption studies. ΔS^0 and ΔH^0 were obtained from the linear regression of $\ln K_d$ versus $1/T$ [36, 38] where K_d was obtained from the distribution coefficient according to the procedure reported in [39] using the experimental Pb^{2+} ion adsorption data.

Recent studies have shown that a proper interpretation of adsorption mechanisms cannot be achieved using the traditional adsorption models (e.g., Sips and Langmuir) due to their parameters usually do not correspond to physicochemical variables for understanding this surface phenomenon [40]. Also, the complex composition of biomaterials could imply the presence of different interaction forces during the adsorption of heavy metal ions thus causing that the fundaments and theory of traditional adsorption models are not satisfied. Considering this fact, statistical physics modeling was implemented to analyze some physicochemical parameters associated with the adsorption mechanism of heavy metal ions on the surfaces of these keratinous biomaterials. This modeling analysis is useful to provide an understanding at macroscopic and microscopic scales of the adsorption system under analysis [41]. The adsorption orientation of heavy metal ions on the surfaces of the keratin-based materials was estimated with a statistical physics model. This statistical physics model assumed that each adsorption site (i.e., carboxyl or amino groups of keratin) of both biomaterials can accept a variable number of heavy metal ions where a monolayer of the adsorbed metal ions was formed on the keratin surface of HH and SF. This model is defined as [41]

$$q_e = \frac{nD}{1 + (C_{hs}/C_e)^n}, \quad (5)$$

where D represents the density of functional groups of the keratin surface involved in the adsorption (mmol/g), C_e is the heavy metal ion concentration at equilibrium (mmol/

Table 1: Main properties of keratin-based biomaterials used in heavy metal removal.

Property	HH	SF
pH	7.9	8.5
Moisture (%)	7.5	8.0
Loss of mass (%)	76.6	97.9
Bulk density (g/cm^3)	0.0725	0.0298

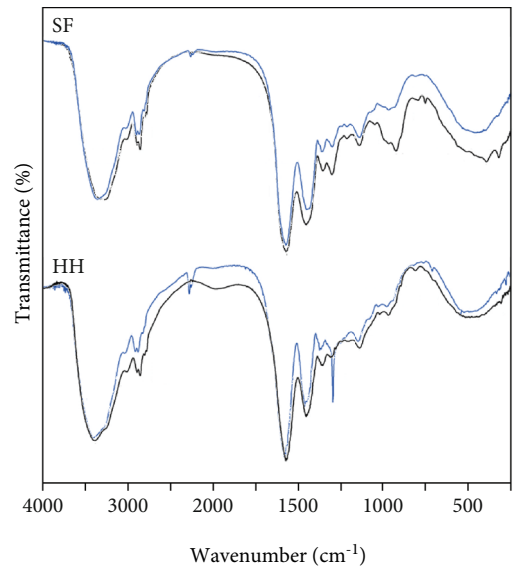

Figure 1: FTIR spectra of keratinous biomaterials applied to remove heavy metals from aqueous solutions. Black line: virgin adsorbent; blue line: metal-loaded adsorbent.

Table 2: Interpretation of infrared spectra of keratinous biomaterials applied in the heavy metal removal.

Description	Wavenumber (cm^{-1})		
	Literature	SF	HH
NH stretching	3295	3308	3422
C-H stretching, $-CH_3$ and $-CH_2-$ asymmetric and symmetric modes	2958	2926	2963
	2847	2853	2930
Amide I (C=O stretch and small contribution from N-H bending)	1637	1649	1655
Amide II (C-H stretching/N-H bending)	1518	1533	1541
Amide III (complex vibration containing O=C=N, C-O, and N-H in-plane bending plus C-N stretching)	1241	1238	1236
Sulphonate (S-O asymmetric stretching)	1175	1154	1177
	1040	1036	1009
Cystine monoxide (R-SO-S-R)	1075	1076	1078

L), n is the number of heavy metal ions adsorbed per functional group available on the keratin surface of HH and SF, and C_{hs} is the heavy metal ion concentration at half-saturation (mmol/L), respectively. Herein, it is convenient to indicate that this statistical physics model has been used to analyze and interpret the adsorption of heavy metal ions in both natural and synthetic adsorbents [42, 43]. Interested readers are referred to the review [41] to understand the fundamentals and formulation of this statistical physics model.

Pb^{2+} ion adsorption data were correlated with the statistical physics model, which was selected as an adsorbate representative of tested heavy metal ions. This modeling approach has been proven to be helpful to provide insights and interpret the adsorption of heavy metal ions using different adsorbents [42–45]. Finally, the adsorption energy (ΔE, kJ/mol) of the Pb^{2+} ion adsorbent surface was calculated with the results of statistical physics models using the next expression [41]:

$$\Delta E = RT \ln\left(\frac{C_{sol}}{C_{hs}}\right), \quad (6)$$

where C_{sol} is the water solubility of the lead nitrate salt (mmol/L) used in the adsorption experiments.

3. Results and Discussion

3.1. Characterization of Keratin-Based Biomaterials. Table 1 displays the main physical properties determined for the two keratin-based biomaterials. pH of these adsorbents was 7.9 and 8.5 for HH and SF, respectively, while their moisture content ranged from 7.5 to 8.0%. Ignition mass losses were 76.6 and 97.9% for HH and SF, and they showed a bulk density of 0.0725 and 0.0298 g/cm^3, respectively.

FTIR spectra of raw and metal-loaded HH and SF are shown in Figure 1, and Table 2 reports the interpretation of their main absorption bands. In general, the absorption spectra of both keratinous biomaterials after and before the adsorption of heavy metal ions were similar. In particular, the absorption band of N-H stretching was observed at 3308–3421 cm^{-1}. The bands appearing in the region of 2926–2962 cm^{-1} were related to symmetrical CH_3 stretching vibration [46]. The band identified at 1649–1655 cm^{-1} was associated with C=O stretching of amide I [47]. The absorption bands of amide II, which were the result of C-H stretching/N-H bending, can be observed at 1533–1541 cm^{-1} [46, 48]. The absorption band of -CO stretching from the -COO- group was identified at ~1390 cm^{-1} [48], and the changes in this band were associated with the interaction of carboxyl groups with heavy metal ions during adsorption. A weak band at 1236–1238 cm^{-1} was identified and linked to the complex vibration containing N-H in-plane, C-O, and O=C=N bending plus C-N stretching, thus showing the presence of amide III [48–50]. The presence of C-S and S-S bonds in these biomaterials can be confirmed with bands at 914–930 cm^{-1} [51]. The absorption band related to the C-S bond was also identified at 640 cm^{-1} [52]. These results proved the protein nature of tested keratinous materials where some changes in the backbone structure of proteins were identified by amides I, II, and III [51].

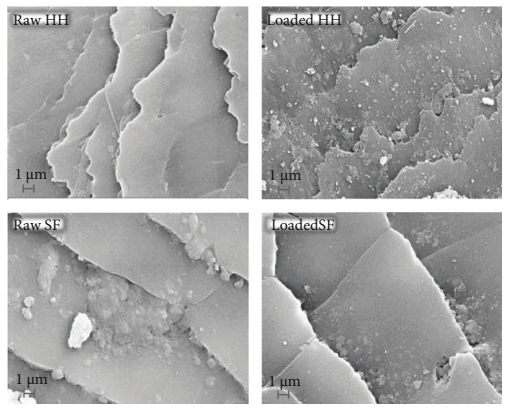

Figure 2: SEM images (×5000) of HH and SF used in the adsorption of heavy metal ions.

SEM micrographs of HH and SF at 5000x magnifications are reported in Figure 2. The surface morphology of these keratinous biomaterials did not present significant differences before and after the removal of heavy metal ions. In general, these biomaterials showed a layer-like surface.

3.2. Adsorption of Heavy Metal Ions using HH and SF at Different Operating Conditions. Adsorption capacities of

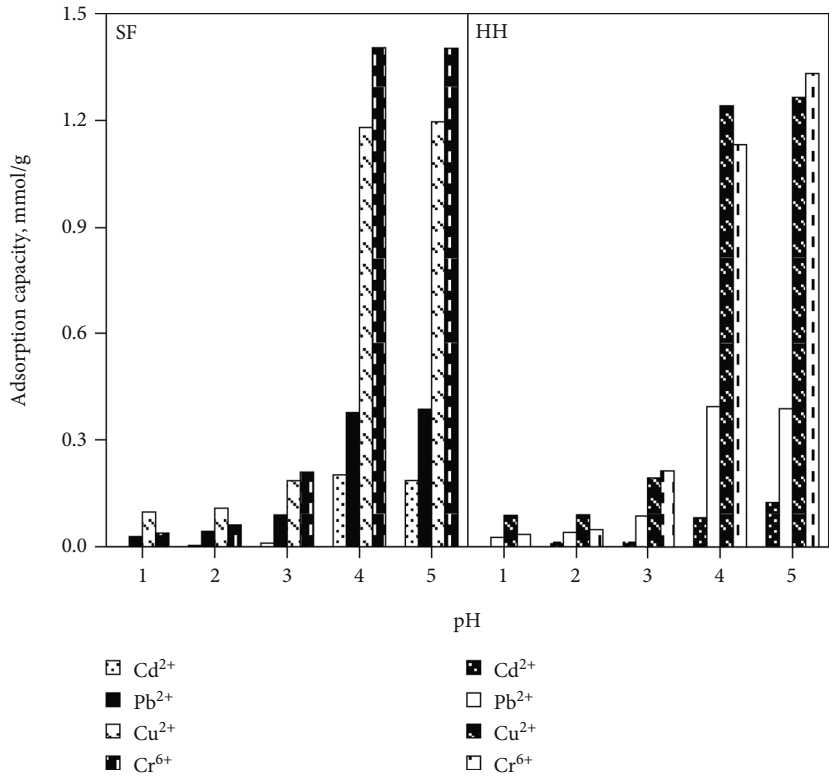

Figure 3: Adsorption of heavy metal ions on SF and HH at 298 K and pH 1–5.

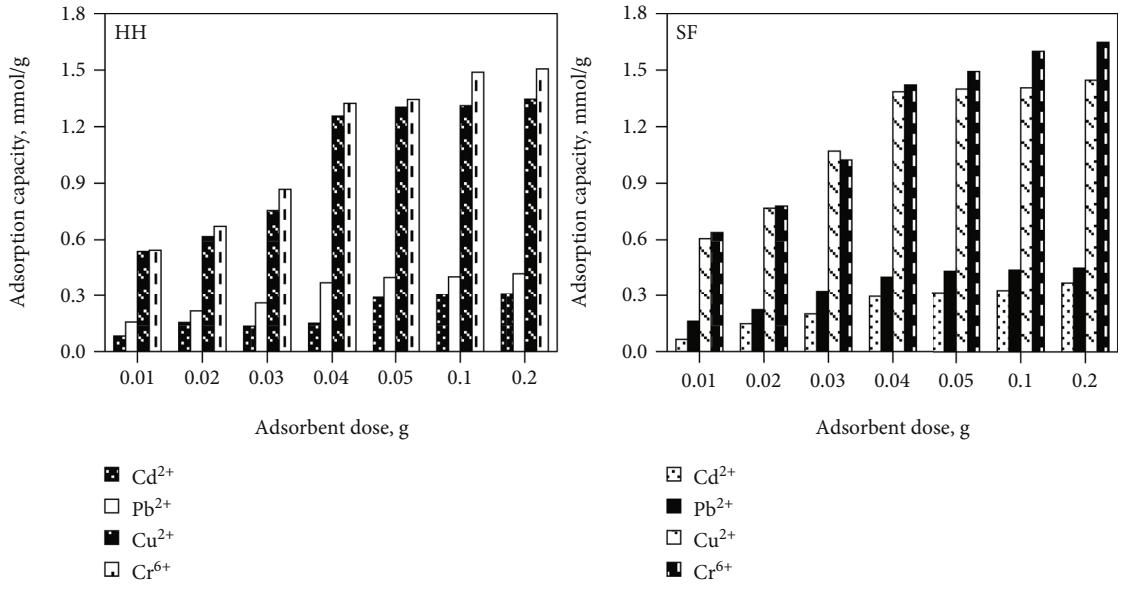

Figure 4: Adsorption of heavy metal ions at different biomaterial doses using (a) HH and (b) SF. Experimental conditions: 298 K and pH 4.

HH and SF can be affected by different operating parameters. In particular, the solution pH was relevant for heavy metal ion removal because it determined the biomaterial surface charge, metal ion solubility, ionization, and speciation [53]. Both SF and HH showed similar adsorption capacities for tested heavy metal ions at different pH conditions where pH 5 corresponded to the maximum removal (see Figure 3). Adsorption capacities of HH ranged from 0.026 to 0.388 mmol/g for Pb^{2+}, 0.088 to 1.264 mmol/g for Cu^{2+}, 0.035 to 1.331 mmol/g for Cr^{6+}, and 0 to 0.125 mmol/g for Cd^{2+} at pH 1-5, while the SF adsorption capacities were 0.028–0.386 mmol/g for Pb^{2+},

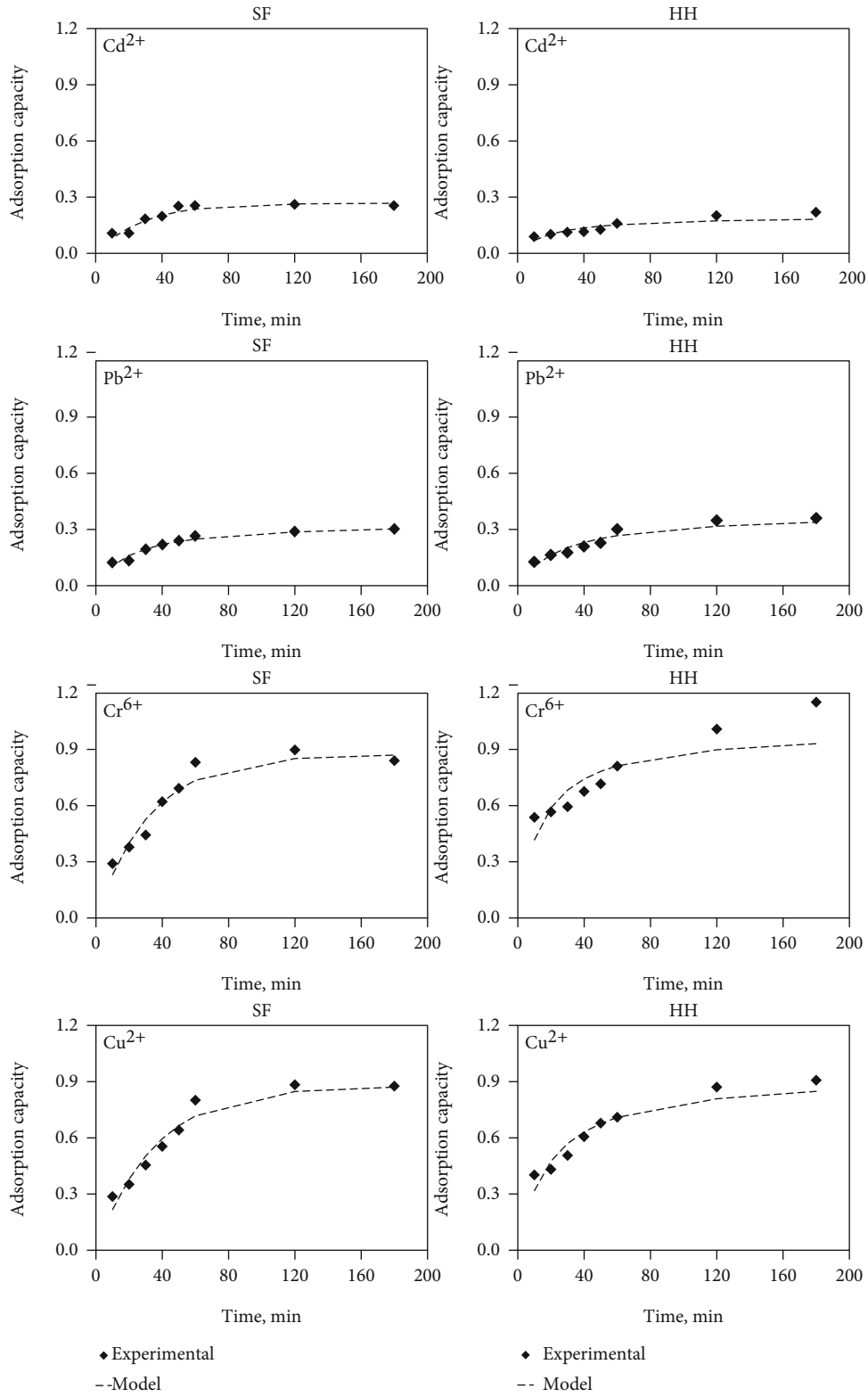

Figure 5: Kinetics of the adsorption of heavy metal ions from aqueous solutions using SF and HH at 298 K and pH 4. Initial metal concentration of 0.48 mmol/L.

0.098-1.196 mmol/g for Cu^{2+}, 0.038-1.402 mmol/g for Cr^{6+}, and 0-0.186 mmol/g for Cd^{2+} at the same operating conditions. All adsorption capacities decreased with solution pH until reaching a minimum value at pH 1 due to the metal ions competed with H^{+} for the functional groups on the keratin surface and the presence of repulsive electrostatic forces generated by the positively charged surfaces of HH and SF.

Table 3: Adsorption kinetic parameters calculated for the removal of Pb^{2+} on HH and SF at 298 K and pH 4.

Adsorbent	Metal	Pseudo-first-order kinetic			Pseudo-second-order kinetic		
		k_1 (min^{-1})	q_e (mmol/g)	R^2	k_2 (g/mmol·min)	q_e (mmol/g)	R^2
SF	Pb^{2+}	0.039	0.287	0.940	0.128	0.343	0.955
	Cd^{2+}	0.035	0.268	0.901	0.117	0.322	0.839
	Cu^{2+}	0.028	0.876	0.951	0.026	1.086	0.940
	Cr^{6+}	0.031	0.873	0.938	0.029	1.070	0.905
HH	Pb^{2+}	0.032	0.327	0.880	0.092	0.391	0.910
	Cd^{2+}	0.042	0.171	0.654	0.261	0.201	0.977
	Cu^{2+}	0.042	0.802	0.833	0.054	0.940	0.916
	Cr^{6+}	0.059	0.846	0.492	0.071	1.003	0.927

The impact of a biomaterial dose on the removal of heavy metal ions is reported in Figure 4. Results showed that the adsorption of these ions depended on this operating parameter where the pollutant removal increased with the biomaterial amount. Note that significant increments in the adsorption capacities were observed from 0.2 to 0.8 g/L where the biomaterial dose impact was less significant at >0.8 g/L. The increment of biomaterial amount increased the number of available functional groups of the keratin surface for the heavy metal ion removal thus generating better adsorption capacities [54, 55].

The adsorption kinetics of Cd^{2+}, Pb^{2+}, Cu^{2+}, and Cr^{6+} ions on tested keratinous materials, using initial concentrations of 0.48 mmol/L at 298 K and pH 4, are reported in Figure 5. Overall, the adsorption capacities of all heavy metal ions for both biomaterials increased with the adsorption time until obtaining the solid-liquid equilibrium. The adsorption of these pollutants implied two stages: (1) a high and rapid initial adsorption of these adsorbates on keratin surface at <50 min and 2) a slower adsorption until reaching the equilibrium and biomaterial saturation at >100 min. The operating time to achieve this adsorption equilibrium was ~100 and 200 min for SF and HH, respectively. Both biomaterials were almost saturated at 100 min of contact time (see Figure 5). Adsorption kinetic modeling is reported in Table 3. The pseudo-first-order model fitted satisfactorily the kinetics of adsorption of heavy metal ions on SF where the adsorption rates ranged from 0.028 to 0.039 min^{-1}. Heavy metal ion kinetic data of HH were correlated satisfactorily with the pseudo-second order model where the calculated adsorption rates were 0.054–0.261 g/mmol·min.

Figure 6 reports the adsorption isotherms of all tested heavy metal ions for both SF and HH at pH 4 and 298 K. These results showed that the initial metal ion concentration increased the metal ion adsorption due to the mass transfer phenomena and a high probability of heavy metal ion-keratin surface interactions. Maximum adsorption capacities were 0.0704-1.4848 mmol/g for HH and 0.0926-1.5658 mmol/g for SF. The highest adsorption was obtained for Cr^{6+} ion using both biomaterials, while Cd^{2+} ion was the pollutant with the lowest adsorption capacities (see Figure 6). It could be expected that the electrostatic forces for the adsorption of Cr^{6+} ion were strongest than those for the other divalent heavy metal ions thus explaining the highest adsorption capacities obtained with both biomaterials.

Pb^{2+} ion was selected as a representative adsorbate of tested heavy metal ions to calculate its corresponding adsorption thermodynamic parameters at 20-50°C using both keratin-based biomaterials. Note that lead is a naturally occurring metal with several industrial applications, and consequently, it has been widely used as an adsorbate to study the removal of this type of pollutants with several materials [3, 4, 8]. Figure 7 shows that the adsorption of this heavy metal ion was endothermic for both HS and SF. The solution temperature is a relevant operating parameter that affected the transport and kinetic processes of heavy metal ion adsorption. Metal ion mobility and swelling effect within the internal structure of the biomaterials were associated with this parameter, and consequently, they affected the adsorption capacities [56]. For instance, the swelling effect can increase the number of functional groups of the keratin surface due to the expanding of microfibrous structure, thus enabling that metal ions can penetrate the biomaterial structure and enhance their removal.

Thermodynamic calculations of Pb^{2+} ion adsorption are reported in Table 4. Note that these thermodynamic parameters were obtained via a data correlation with $R^2 > 0.97$. All calculated ΔG^0 values were negative indicating that Pb^{2+} ion adsorption on SF and HH was a thermodynamically spontaneous process. Note that the spontaneity degree of adsorption of Pb^{2+} ions increased with temperature. ΔH^0 values corresponded to an endothermic adsorption for both keratin-based biomaterials where the presence of both chemical and physical attraction forces could be expected [57]. Note that energy was required for the adsorbate to transfer through solution to the adsorption sites of keratin and get stripped out of their hydration shell [58]. ΔS^0 for Pb^{2+} ion adsorption was 0.34 and 0.29 kJ/mol for SF and HH, respectively. These positive values were an indication of increased disorderliness at the biomaterial-liquid interface during the removal of these heavy metal ions, which could imply a dehydration of adsorbate before getting into the functional groups of biomaterials [59].

Finally, a comparison of the performance of these keratinous biomaterials with respect to other adsorbents used in the removal of heavy metal ions is provided in Table 5.

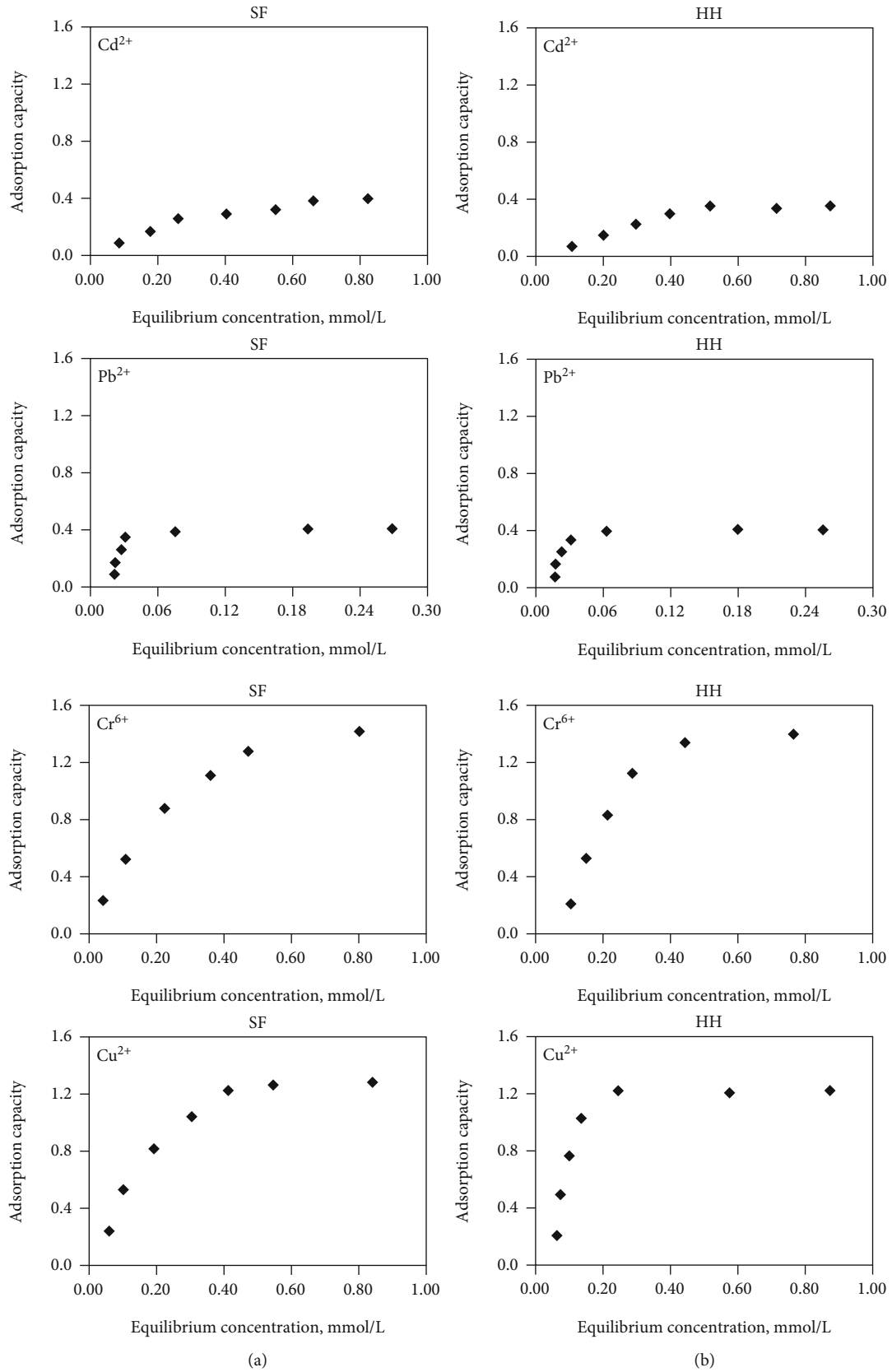

Figure 6: Isotherms of the adsorption of heavy metal ions from aqueous solutions using (a) SF and (b) HH at pH 4 and 298 K.

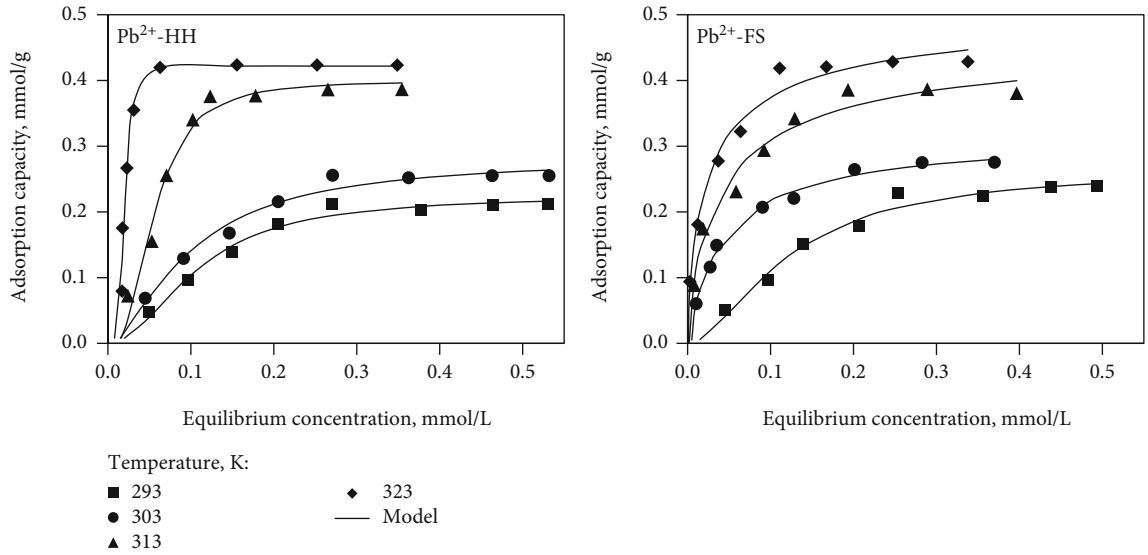

Figure 7: Isotherms of Pb^{2+} adsorption on HH and SF at pH 4 and their statistical physics modeling.

Table 4: Thermodynamic parameters for the Pb^{2+} adsorption on SF and HH at pH 4.

Adsorbent	ΔH^0 (kJ/mol)	ΔS^0 (kJ/mol)	ΔG^0 (kJ/mol)			
			293 K	303 K	313 K	323 K
SF	97.1	0.34	-0.39	-6.11	-7.86	-10.89
HH	84.5	0.29	-0.43	-1.59	-4.25	-9.28

Overall, HH and SF showed a competitive performance for the heavy metal ion removal, and they can outperform the adsorption capacities reported for different adsorbents. For instance, the Pb^{2+} and Cr^{6+} adsorption capacities of HH and SF were higher than those of a cysteine-modified biomass [60] and surfactant-modified coconut coir [61]. As stated, HH and SF are renewable and low-cost biomaterials thus offering additional advantages for their application in the water treatment.

Herein, it is convenient to remark that these biomaterials can be regenerated using acidic solutions to desorb the heavy metal ions loaded in their surfaces. This approach will allow the recovery of the adsorption properties of these adsorbents thus offering the possibility of reducing the costs of their application in water treatment. The spent biomaterial after reaching its lifetime should be properly disposed to avoid additional environmental pollution, or alternatively, they could be employed as a feedstock in other industrial processes (e.g., the manufacturing of polymer-based materials). Further studies in this direction are required to establish the best alternative for the final disposal of these biomaterials used in the adsorption of heavy metal ions.

3.3. Statistical Physics Calculations and Interpretation of the Adsorption Mechanism. Figure 7 also shows the results of statistical physics calculations for the Pb^{2+} ion adsorption isotherms of both HH and SF where $R^2 = 0.998$ was obtained. Table 6 reports the physicochemical parameters calculated with the statistical physics model, which were utilized to complement the analysis of the Pb^{2+} ion adsorption mechanism.

Statistical physics calculations indicated the parameter $n > 1$ for the Pb^{2+} ion adsorption on HH. This result suggested that the adsorption of this metal ion on this keratinous biomaterial could be a multi-ionic process where Pb^{2+} ions interacted with one functional group from the keratin surface. For the case of SF, the values of this parameter ranged from 0.5 to 1 indicating that this heavy metal could be adsorbed on the SF surface via the interaction with one and two functional groups from keratin at the same time. The calculated density of functional groups of HH and SF surfaces that could be involved in the adsorption was 0.092-0.700 mmol/g at tested conditions. The calculated adsorption capacities of Pb^{2+} ion to achieve the biomaterial saturation (q_{max}) were 0.224-0.421 mmol/g for HH and 0.264-0.511 mg/g for SF. On the other hand, calculated adsorption energies ranged from 23.6 to 30.4 kJ/mol and from 23.3 to 30.0 kJ/mol for HH and SF, respectively. These calculations confirmed the endothermic nature of this adsorption process [41]. These adsorption energy values were consistent with the typical values of electrostatic interactions (10–50 kJ/mol) and coordination exchange (40 kJ/mol), which were the expected forces related to the adsorption mechanism of heavy metal ions with these biomaterials [36]. In particular, the adsorption of heavy metal ions on SF and HH surfaces can be represented by the next expressions:

$$\begin{aligned} &\blacksquare\equiv\text{Keratin} - (NH_3{\bullet}OH)_2 + M^{2+} \leftrightarrow \blacksquare \equiv \text{Keratin} - (NH_2)_2M(OH)_2 + 2H^+, \\ &\blacksquare\equiv\text{Keratin} - [COOH]_2 + M^{2+} \leftrightarrow \blacksquare \equiv \text{Keratin} - (COO)_2M + 2H^+, \end{aligned} \quad (7)$$

where carboxyl and amino groups of keratin are expected to be involved in the adsorption of heavy metal ions [36, 41].

Table 5: Adsorption capacities of different materials reported for the heavy metal removal.

Adsorbent	Metal	Experimental conditions		q_e (mmol/g)	Reference
		pH	Temperature (°C)		
Dried activated sludge	Cd^{2+}	6	25	0.75	[57]
	Pb^{2+}	4	25	0.64	
Cystine modified biomass	Cd^{2+}	<6	25	0.10	[58]
	Pb^{2+}	<6	25	0.22	
Green algae spirogyra	Pb^{2+}	5	25	0.68	[59]
Protonated rice bran	Ni^{2+}	6	30	0.77	[60]
Surfactant modified coconut coir	Cr^{6+}	2	32	1.47	[61]
Coffee powder	Fe^{3+}	5.5-6	25	1.53	[62]
Tea powder	Fe^{3+}	5.5-6	25	5.10	[62]
Dried activated sludge	Fe^{3+}	7	20	0.06	[63]
Non living cells of *Chlorella vulgaris*	Cd^{2+}	NR	25	0.40	[64]
	Cu^{2+}	NR	25	0.90	
	Pb^{2+}	NR	25	0.30	
This work: SF	Pb^{2+}	4	30	0.28	
This work: HH	Pb^{2+}	4	30	0.26	

Nomenclature: NR - not reported

Table 6: Calculated statistical physics parameters for the Pb^{2+} adsorption on HH and SF at pH 4.

Adsorbent	T (K)	n	D (mmol/g)	q_{max} (mmol/g)	ΔE (kJ/mol)
HH	293	2	0.112	0.224	23.6
	303	1.58	0.174	0.275	24.5
	313	2.65	0.151	0.399	26.8
	323	4.57	0.092	0.421	30.4
SF	293	1.71	0.154	0.264	23.3
	303	0.96	0.337	0.324	26.6
	313	0.81	0.574	0.465	27.7
	323	0.73	0.700	0.511	30.0

4. Conclusions

The thermodynamics and mechanism interpretation of the adsorption of heavy metal ions on human hair and sheep were analyzed and discussed. These keratin-based biomaterials achieved adsorption capacities up to 1.4 mmol/g for the heavy metal ion removal from aqueous solutions. Both biomaterials showed the highest adsorption capacities for chromium ions (1.48 and 1.57 mmol/g with HH and SF, respectively), while the lowest adsorption capacities were obtained for cadmium ions (0.07 and 0.09 mmol/g with HH and SF, respectively). Adsorption of heavy metal ions with both keratinous materials was highly pH dependent, and the adsorption capacities were reduced up to 98% at pH 1. A detailed analysis of lead ion adsorption was performed, and results indicated that the removal of this heavy metal ion was endothermic for both biomaterials with adsorption enthalpies of 85–97 kJ/mol. Statistical physics calculations suggested the occurrence of a multi-ion process in lead ion adsorption especially for human hair and confirmed the endothermic nature of this removal process. These biomaterials showed competitive adsorption capacities and can outperform commercial activated carbons and other adsorbents reported in literature. Therefore, they are an alternative to prepare composites and functionalized materials for achieving the goal of a low-cost and sustainable wastewater treatment.

Data Availability

Data of this paper are available on request to the corresponding author.

Conflicts of Interest

The authors declared no potential conflicts of interest with respect to the research, authorship, and/or publication of this article.

Acknowledgments

MB acknowledges the financial support through the COMETE project (COnception in silico de Matériaux pour l'EnvironnemenT et l'Energie) cofunded by the European Union under the program "FEDER-FSE Lorraine et Massif des Vosges 2014-2020." ABP is also thankful to the University of Lorraine for the invited professorship in the academic year 2020-2021.

References

[1] F. J. Cervantes, S. G. Pavlostathis, and A. C. Van Haandel, *Advanced Biological Treatment Processes for Industrial Wastewaters: Principles and Applications*, IWA publishing, London, 1st edition, 2006.

[2] I. Mironyuk, T. Tatarchuk, H. Vasylyeva, V. M. Gun'ko, and I. Mykytyn, "Effects of chemosorbed arsenate groups on the mesoporous titania morphology and enhanced adsorption properties towards Sr(II) cations," *Journal of Molecular Liquids*, vol. 282, pp. 587–597, 2019.

[3] A. K. Meena, K. Kadirvelu, G. K. Mishraa, C. Rajagopal, and P. N. Nagar, "Adsorption of Pb(II) and Cd(II) metal ions from aqueous solutions by mustard husk," *Journal of Hazardous Materials*, vol. 150, pp. 619–625, 2008.

[4] Y. Cao, H. A. Dhahad, H. M. Hussen et al., "Adsorption properties of two-dimensional carbon material towards the heavy metal ions," *Journal of Molecular Liquids*, vol. 342, p. 117500, 2021.

[5] A. Q. Selim, L. Sellaoui, S. A. Ahmed et al., "Statistical physics-based analysis of the adsorption of Cu^{2+} and Zn^{2+} onto synthetic cancrinite in single compound and binary systems," *Journal of Environmental Chemical Engineering*, vol. 7, p. 103217, 2019.

[6] T. S. Jamil, H. S. Ibrahim, I. H. Abd El-Maksoud, and S. T. El-Wakeel, "Application of zeolite prepared from Egyptian kaolin for removal of heavy metals: I. Optimum conditions," *Desalination*, vol. 258, pp. 34–40, 2010.

[7] M. K. Seliem and S. Komarneni, "Equilibrium and kinetic studies for adsorption of iron from aqueous solution by synthetic Na-A zeolites: statistical modeling and optimization," *Microporous and Mesoporous Materials*, vol. 228, pp. 266–274, 2016.

[8] C. Liu, Q. Wang, F. Jia, and S. Song, "Adsorption of heavy metals on molybdenum disulfide in water: a critical review," *Journal of Molecular Liquids*, vol. 292, p. 111390, 2019.

[9] M. Balsamo, F. Di Natale, A. Erto, and F. Montagnaro, "Coal combustion ash sorbents for Cd and Zn capture in single-compound and binary systems," *Desalination and Water Treatment*, vol. 127, pp. 41–49, 2018.

[10] A. E. Burakov, E. V. Galunina, I. V. Burakova et al., "Adsorption of heavy metals on conventional and nanostructured materials for wastewater treatment purposes: a review," *Ecotoxicology and Environmental Safety*, vol. 148, pp. 702–712, 2018.

[11] D. Vilela, J. Parmar, Y. Zeng, Y. Zhao, and S. Sánchez, "Graphene-based microbots for toxic heavy metal removal and recovery from water," *Nano Letters*, vol. 16, pp. 2860–2866, 2016.

[12] P. Kar and M. Misra, "Use of keratin fiber for separation of heavy metals from water," *Journal of Chemical Technology and Biotechnology*, vol. 79, pp. 1313–1319, 2004.

[13] E. Fosso-Kankeu, A. Webster, I. O. Ntwampe, and F. B. Waanders, "Coagulation/flocculation potential of polyaluminium chloride and bentonite clay tested in the removal of methyl red and crystal violet," *Arabian Journal for Science and Engineering*, vol. 42, pp. 1389–1397, 2017.

[14] T. P. Madhavi, M. Srimurali, and K. N. Prasad, "Color removal from industrial wastewater using alum," *Journal of Environmental Research And Development*, vol. 8, pp. 890–894, 2014.

[15] T. A. Egloffstein, "Natural bentonites – influence of the ion exchange and partial desiccation on permeability and self-healing capacity of bentonites used in GCLs," *Geotextiles and Geomembranes*, vol. 19, pp. 427–444, 2001.

[16] S. A. Nabi, M. Shahadat, R. Bushra, A. H. Shalla, and A. Azam, "Synthesis and characterization of nano-composite ion-exchanger; its adsorption behavior," *Colloids and Surfaces. B, Biointerfaces*, vol. 87, pp. 122–128, 2011.

[17] L. Narayanasamy and T. Murugesan, "Degradation of alizarin yellow R using UV/H_2O_2 advanced oxidation process," *Environmental Progress & Sustainable Energy*, vol. 33, pp. 482–489, 2014.

[18] M. S. Lucas and J. A. Peres, "Decolorization of the azo dye reactive black 5 by Fenton and photo-Fenton oxidation," *Dyes and Pigments*, vol. 71, pp. 236–244, 2006.

[19] E. Kusvuran, O. Gulnaz, S. Irmak, O. M. Atanur, H. I. Yavuz, and O. Erbatur, "Comparison of several advanced oxidation processes for the decolorization of Reactive Red 120 azo dye in aqueous solution," *Journal of Hazardous Materials*, vol. 109, pp. 85–93, 2004.

[20] J. S. B. Melbiah, D. Nithya, and D. Mohan, "Surface modification of polyacrylonitrile ultrafiltration membranes using amphiphilic Pluronic F127/$CaCO_3$ nanoparticles for oil/water emulsion separation," *Colloids and Surfaces A: Physicochemical and Engineering Aspects*, vol. 516, pp. 147–160, 2017.

[21] B. Wu, T. Christen, H. Sin et al., "Improved performance of gravity-driven membrane filtration for seawater pretreatment: implications of membrane module configuration," *Water Research*, vol. 114, pp. 59–68, 2017.

[22] F. Senusi, M. Shahadat, S. Ismail, and S. A. Hamid, "Recent advancement in membrane technology for water purification," in *Modern Age Environmental Problems and Their Remediation*, M. Oves, M. Z. Khan, and I. M. I. Ismail, Eds., pp. 147–167, Springer, Cham, New York, 2018.

[23] J. M. Dickhout, J. Moreno, P. M. Biesheuvel, L. Boels, R. G. H. Lammertink, and W. M. de Vos, "Produced water treatment by membranes: a review from a colloidal perspective," *Journal of Colloid and Interface Science*, vol. 487, pp. 523–534, 2017.

[24] L. Fan, Y. Zhou, W. Yang, G. Chen, and F. Yang, "Electrochemical degradation of aqueous solution of Amaranth azo dye on ACF under potentiostatic model," *Dyes and Pigments*, vol. 76, pp. 440–446, 2008.

[25] D. Rajkumar, B. J. Song, and J. G. Kim, "Electrochemical degradation of reactive blue 19 in chloride medium for the treatment of textile dyeing wastewater with identification of intermediate compounds," *Dyes and Pigments*, vol. 72, pp. 1–7, 2007.

[26] A. Fernandes, A. Morão, M. Magrinho, A. Lopes, and I. Gonçalves, "Electrochemical degradation of C. I. Acid Orange 7," *Dyes and Pigments*, vol. 61, pp. 287–296, 2004.

[27] A. O. Salaudeen, "Biosorption of heavy metals from aqueous solutions: an insight and review," *International Journal of Soil, Sediment and Water*, vol. 14, pp. 835–891, 2021.

[28] G. F. Coelho, A. C. Goncalves Jr., C. R. T. Tarley, J. Casarin, H. Nacke, and M. A. Francziskowski, "Removal of metal ions Cd (II), Pb (II), and Cr (III) from water by the cashew nut shell _Anacardium occidentale_ L," *Ecological Engineering*, vol. 73, pp. 514–525, 2014.

[29] C. Santhosh, V. Velmurugan, G. Jacob, S. K. Jeong, A. N. Grace, and A. Bhatnagar, "Role of nanomaterials in water treatment applications: a review," *Chemical Engineering Journal*, vol. 306, pp. 1116–1137, 2016.

[30] S. P. Mishra, "Adsorption-desorption of heavy metal ions," *Current Science*, vol. 107, pp. 601–612, 2014.

[31] R. Bisht, M. Agarwal, and K. Singh, "Heavy metal removal from wastewater using various adsorbents: a review," *Journal of Water Reuse and Desalination*, vol. 7, pp. 387–419, 2016.

[32] R. O. Cañizares-Villanueva, "Biosorption of heavy metals using microbial biomass," *Revista Latinoamericana de Microbiología*, vol. 42, pp. 131–143, 2000.

[33] R. K. Gautam, S. K. Sharma, S. Mahiya, and M. C. Chattopadhyaya, "Heavy metals in water: presence, removal and safety," in *Contamination of Heavy Metals in Aquatic Media: Transport, Toxicity and Technologies for Remediation*, S. Sharma, Ed., pp. 1–24, Royal Society of Chemistry, United Kingdom, 2014.

[34] S. Saha, M. Zubair, M. A. Khosa, S. Song, and A. Ullah, "Keratin and chitosan biosorbents for wastewater treatment: a review," *Journal of Polymers and the Environment*, vol. 27, pp. 1389–1403, 2019.

[35] E. D. Revellame, D. L. Fortela, W. Sharp, R. Hernandez, and M. E. Zappi, "Adsorption kinetic modeling using pseudo-first order and pseudo-second order rate laws: a review," *Cleaner Engineering and Technology*, vol. 1, p. 100032, 2020.

[36] E. C. Lima, A. A. Gomes, and H. N. Tran, "Comparison of the nonlinear and linear forms of the van't Hoff equation for calculation of adsorption thermodynamic parameters (ΔS^0 and ΔH^0)," *Journal of Molecular Liquids*, vol. 311, p. 113315, 2020.

[37] Y. Sağ and T. Kutsal, "The selective biosorption of chromium (VI) and copper (II) ions from binary metal mixtures by *R. arrhizus*," *Process Biochemistry*, vol. 31, pp. 561–572, 1996.

[38] A. O. Salaudeen, F. W. Abdulrahman, H. D. Aliyu, and H. Yakubu, "Biosorption of Pb(II) and Cu(II) from aqueous solution using chicken feather: thermodynamics and mass balance studies," *Asian Journal of Applied Chemistry Research*, vol. 1, pp. 1–9, 2018.

[39] H. N. Tran, S. J. You, A. Hosseini-Bandegharaei, and H. P. Chao, "Mistakes and inconsistencies regarding adsorption of contaminants from aqueous solutions: a critical review," *Water Research*, vol. 120, pp. 88–116, 2017.

[40] J. N. Putro, S. P. Santoso, S. Ismadji, and Y. H. Ju, "Investigation of heavy metal adsorption in binary system by nanocrystalline cellulose - bentonite nanocomposite: improvement on extended Langmuir isotherm model," *Microporous and Mesoporous Materials*, vol. 246, pp. 166–177, 2017.

[41] O. Amrhar, L. El Gana, and M. Mobarak, "Calculation of adsorption isotherms by statistical physics models: a review," *Environmental Chemistry Letters*, vol. 19, no. 6, pp. 4519–4547, 2021.

[42] F. Dhaouadi, L. Sellaoui, M. Badawi et al., "Statistical physics interpretation of the adsorption mechanism of Pb^{2+}, Cd^{2+} and Ni^{2+} on chicken feathers," *Journal of Molecular Liquids*, vol. 319, p. 114168, 2020.

[43] L. Sellaoui, J. Ali, M. Badawi, A. Bonilla-Petriciolet, and Z. Chen, "Understanding the adsorption mechanism of Ag^+ and Hg^{2+} on functionalized layered double hydroxide via statistical physics modeling," *Applied Clay Science*, vol. 198, p. 105828, 2020.

[44] A. Yazidi, L. Sellaoui, M. Badawi et al., "Ternary adsorption of cobalt, nickel and methylene blue on a modified chitin: phenomenological modeling and physical interpretation of the adsorption mechanism," *International Journal of Biological Macromolecules*, vol. 158, pp. 595–604, 2020.

[45] L. Sellaoui, E. P. Hessou, M. Badawi et al., "Trapping of Ag^+, Cu^{2+}, and Co^{2+} by faujasite zeolite Y: new interpretations of the adsorption mechanism via DFT and statistical modeling investigation," *Chemical Engineering Journal*, vol. 420, p. 127712, 2021.

[46] N. Eslahi, F. Dadashian, and N. H. Nejad, "An investigation on keratin extraction from wool and feather waste by enzymatic hydrolysis," *Preparative Biochemistry & Biotechnology*, vol. 43, pp. 624–648, 2013.

[47] A. Aluigi, M. Zoccola, C. Vineis, C. Tonin, F. Ferrero, and M. Canetti, "Study on the structure and properties of wool keratin regenerated from formic acid," *International Journal of Biological Macromolecules*, vol. 41, pp. 266–273, 2007.

[48] T. Nikiforova, V. Kozlov, and M. Islyaikin, "Sorption of d-metal cations by keratin from aqueous solutions," *Journal of Environmental Chemical Engineering*, vol. 7, p. 103417, 2019.

[49] A. Vasconcelos, G. Freddi, and A. Cavaco-Paulo, "Biodegradable materials based on silk fibroin and keratin," *Biomacromolecules*, vol. 9, pp. 1299–1305, 2008.

[50] J. Zhang, Y. Li, J. Li et al., "Isolation and characterization of biofunctional keratin particles extracted from wool wastes," *Powder Technology*, vol. 246, pp. 356–362, 2013.

[51] B. Ma, X. Qiao, X. Hou, and Y. Yang, "Pure keratin membrane and fibers from chicken feather," *International Journal of Biological Macromolecules*, vol. 89, pp. 614–621, 2016.

[52] Y. Estévez-Martínez, C. Velasco-Santos, A. L. Martínez-Hernández et al., "Grafting of multiwalled carbon nanotubes with chicken feather keratin," *Journal of Nanomaterials*, vol. 2013, 2013.

[53] R. Nadeem, M. A. Hanif, F. Shaheen, S. Perveen, M. N. Zafar, and T. Iqbal, "Physical and chemical modification of distillery sludge for Pb (II) biosorption," *Journal of Hazardous Materials*, vol. 150, pp. 335–342, 2008.

[54] R. Razmouski and M. Sciban, "Biosorption of Cr (VI) and Cu(II) by waste tea fungal biomass," *Ecological Engineering*, vol. 34, pp. 179–186, 2008.

[55] S. Karthikeyan, R. Balasubramanian, and C. S. P. Yer, "Evaluation of the marine algae *Ulva fasciata* and *Sargassum sp*. for the biosorption of Cu(II) from aqueous solutions," *Bioresource Technology*, vol. 98, pp. 452–455, 2007.

[56] C. K. Jain, "Adsorption of zinc onto bed sediments of the River Ganga; adsorption models and kinetics," *Hydrological Sciences Journal*, vol. 46, pp. 419–434, 2001.

[57] M. Horsfall, A. I. Spiff, and A. A. Abia, "Studies on the influence of mercaptoacetic acid (MAA) modification of cassava (*Manihot sculenta* cranz) waste biomass on the adsorption of Cu^{2+} and Cd^{2+} from aqueous solution," *Bulletin of the Korean Chemical Society*, vol. 25, pp. 969–976, 2004.

[58] K. L. Wasewar, "Adsorption of metals onto tea factory waste," *International Journal of Applied Science-Research and Review*, vol. 3, pp. 303–322, 2010.

[59] V. Vadivelan and K. V. Kumar, "Equilibrium, kinetics, mechanism, and process design for the sorption of methylene blue onto rice husk," *Journal of Colloid and Interface Science*, vol. 286, pp. 90–100, 2005.

[60] J. Yu, M. Tong, X. Sun, and B. Li, "Cystine-modified biomass of Cd(II) and Pb(II) biosorption," *Journal of Hazardous Materials*, vol. 143, pp. 277–284, 2007.

[61] C. Namasivayam and M. V. Sureshkumar, "Removal of chromium (VI) from water and wastewater using surfactant modified coconut coir pith as biosorbent," *Bioresource Technology*, vol. 99, pp. 2218–2225, 2008.

[62] X. Wang, S. Xia, L. Chen, J. Zhao, J. Chovelon, and J. Nicole, "Biosorption of Cd(II) and Pb(II) ions from aqueous solutions onto dried activated sludge," *Journal of Environmental Sciences*, vol. 18, pp. 840–844, 2006.

[63] V. K. Gupta and V. A. Rastogi, "Biosorption of Pb from aqueous solutions by green alga *Spirogyra* species: kinetics and equilibrium studies," *Journal of Hazardous Materials*, vol. 152, pp. 407–414, 2008.

[64] N. M. Zafar, R. Nadeem, and M. A. Hanif, "Biosorption of nickel from protonated rice bran," *Journal of Hazardous Materials*, vol. 143, no. 1-2, pp. 478–485, 2007.

[65] K. M. Elsherif, A. El-Hashani, and I. Haider, "Biosorption of Fe (III) onto coffee and tea powder: equilibrium and kinetic study," *Asian Journal of Green Chemistry*, vol. 2, pp. 380–394, 2018.

[66] R. Shokoohi, M. H. Saghi, H. R. Ghafari, and M. Hadi, "Biosorption of iron from aqueous solution by dried biomass of activated sludge," *Journal of Environmental Health Science & Engineering*, vol. 6, pp. 107–114, 2009.

[67] M. H. Ali, A. E. M. Hussian, A. M. Abdel-Satar, M. E. Goher, A. Napiórkowska-Krzebietke, and A. M. A. El-Monem, "The isotherm and kinetic studies of the biosorption of heavy metals by non-living cells of *Chlorella vulgaris*," *Journal of Elementology*, vol. 21, pp. 1263–1276, 2016.